Available online at www.sciencedirect.com
SCIENCE DIRECT
Thin Solid Films 490 (2005) 118 – 123
thin solid films
www.elsevier.com/locate/tsf

Effect of SnO_2 on the photocatalytical properties of TiO_2 films

Arturo I. Martínez[a,*], Dwight R. Acosta[a], Gerardo Cedillo[b]

[a]Instituto de Física, Universidad Nacional Autónoma de México, A.P. 20-364, 01000 México D.F.
[b]Instituto de Investigaciones en Materiales, Universidad Nacional Autónoma de México, México, D.F. 01000, México

Available online 20 June 2005

Abstract

TiO_2/SnO_2 thin films with different tin atomic percentages were successfully prepared on glass substrates by the spray pyrolysis method from an alcoholic solution of $TiO[C_5H_7O_2]_2$ with different concentrations of $SnCl_4$. The TiO_2/SnO_2 thin films prepared at 450 °C presented the anatase phase in polycrystalline configuration from %Sn=0 in the starting solution up to %Sn=20, at higher tin content the films present an amorphous configuration. The resulting thin films have a homogeneous surface structure with some porosity. The photocatalytical properties of the films were evaluated with the degradation of methylene blue. The products of the degradation reaction were identified by ^1H nuclear magnetic resonance and the film properties were studied by atomic force microscopy, scanning electron microscopy, UV–Vis spectroscopy, and X-ray diffraction.

Keywords: Titanium oxide; Spray pyrolysis; Photocatalysis

1. Introduction

TiO_2 thin films have different practical applications and are used in: photocatalysis [1], gas sensors [2], capacitors [3], electrochromic devices [4], and materials protection [5]. Also due to their excellent biocompatibility and hemocompatibility, they are useful in the medical–biological field [6]. TiO_2 can be found in three different crystal phases: brookite, anatase and rutile. Tetragonal phases (anatase and rutile) have been found in thin films deposited by sputtering, spray pyrolysis, and sol–gel methods [7]. The orthorhombic phase (brookite) is commonly found in TiO_2 thin films prepared by sol–gel under specific hydrothermal conditions and/or in the presence of small amounts of sodium [7]. Although the anatase phase is less stable than rutile from a thermodynamic point of view, its formation is kinetically favored at temperatures lower than 600 °C. This phase offers a high surface area and a high density of active sites for adsorption. Moreover, it has been found that this is the most active phase for photocatalytic applications [1]. The use of wide band gap semiconductors as photocatalysts is a subject of continuous research due to the need to decrease the amount of chemical wastes from water and air. However, for environmental purposes, the semiconductor materials based on titanium oxide are of greater interest than other semiconductors [8,9]. Nevertheless, for practical applications, it is necessary to improve their photocatalytic activity (PA). Several methods have been developed to increase the PA of TiO_2, such as: the adsorption of noble metals on the TiO_2 surface, the increase in the TiO_2 surface area and the preparation of semiconductor alloys [10]. Also, the PA can be increased using coupled semiconductor particles [11]. Li and co-workers [12], for instance, found that the new semiconductor alloy TiO_2 based on an optimal WO_x amount achieved a higher photocatalytic activity than the pure TiO_2 photocatalyst for the degradation of methylene blue. Lin and co-workers [13] have found that Sn(IV) substitution for Ti(IV) in rutile TiO_2 increases the PA of titanium oxide powders up to 15 times for the degradation of acetone. Zheng and coworkers [14] were able to increase the TiO_2 photocatalytic activity in the degradation of rhodamine B dye by the implantation of tin ions into TiO_2 films. Also the results of Cao et al. show an improvement of the PA of titanium oxide by doping the anatase lattice with Sn^{4+} ions

* Corresponding author.
E-mail address: artmtz@correo.unam.mx (A.I. Martínez).

0040-6090/$ - see front matter © 2005 Elsevier B.V. All rights reserved.
doi:10.1016/j.tsf.2005.04.060

in thin films prepared by plasma enhanced chemical vapor deposition [15].

TiO_2/SnO_2 thin films with different amounts of SnO_2 have been studied in this work. The effects of tin on the structural, optical, morphological, and photocatalytical properties of TiO_2 thin films prepared by spray pyrolysis have been studied. Using electron microscopy and optical measurements, it has been found that the prepared TiO_2/SnO_2 samples exhibit a greater porosity and smaller band gap energies than those of pure TiO_2 thin films. Following arguments mentioned in the literature we propose that the occurrence of changes in the electronic structure related to the presence of impurity levels below of the TiO_2 conduction band corresponding to both Sn^{4+} states and to the conduction band of the SnO_2 phase the optical band gap decrease with the tin content [11,15]. The improvement of the PA exhibit by TiO_2/SnO_2 thin films is a direct consequence of the existence of more adsorption sites than those exhibited by TiO_2 films and the existence of smaller energy gap which will favor the generation of more electron-hole pairs than those generated in TiO_2 films when illuminated with UV radiation. Also, the introduction of SnO_2 to the TiO_2 lattice produces a more efficient separation of the photo generated pairs [11,15].

2. Experimental procedure

The deposition of the TiO_2/SnO_2 thin films was done by spraying alcoholic solutions of 0.15 M titanium (IV) oxide acetyl acetonate $TiO[C_5H_7O_2]_2$ (TiOAA) with different amounts of $SnCl_4$; the concentration of tin in the solution was calculated using the following formula $\%Sn = \{[Sn^{4+}]/([Sn^{4+}]+[Ti^{4+}])\} \times 100$, %Sn takes values of 0, 5, 9, 13, 17, 20, and 40. The corresponding solutions were sprayed with a glass atomizer on glass substrates heated by an aluminum hot plate with a solution flow rate of 4.7 mL/s. Filtered compressed air at a pressure of 20 psi was used as carrier gas. To avoid rapid cooling of the substrate, the spraying process consisted in spraying cycles of 1 s followed by short periods without spray of 25 s; keeping a substrate temperature (T_s) of 450±5 °C. The whole system was enclosed within a chamber provided with a gas extractor system that removes the vapors produced by the pyrolytical reaction.

The crystalline structure of the films was characterized using a Bruker AXS D8 Advance X-ray diffractometer, with a Cu K_α ($\lambda = 0.15405$ nm) radiation source. The surface morphology was observed using a JEOL 5900LV scanning electron microscope (SEM) and an atomic force microscope (AFM) JSPM-5200 from JEOL. AFM studies were made at ambient conditions in tapping mode using a commercial silicon cantilever with a spring constant of 40 N/m. The thickness of the films was measured with a profile meter alpha-Step 100; the measured steps were made during the deposition process by blocking a part of the substrate with a small piece of glass. The UV–Visible spectra of the films were obtained using an Agilent 8453 UV–Visible spectrophotometer. Compositional studies were done with energy dispersive X-ray spectroscopy (EDS) attached to a JEOL 5900LV SEM. The photocatalytic tests were run in a homemade photoreactor and the degradation products of the photocatalytic reaction were identified with a nuclear magnetic resonance (NMR) spectrometer Bruker Avance 400.

The photocatalytic properties of the prepared films were studied by the decomposition of methylene blue (MB), ($C_{16}H_{18}N_3S{\cdot}Cl{\cdot}3H_2O$). Glass, TiO_2, or TiO_2/SnO_2 coatings of 4 cm^2 were immersed in a batch reactor containing 10 mL of a 30 μM aqueous MB solution and were irradiated with UV light from a lamp with a very low intensity of 6 W and operating at 3.25 and 3.39 eV. The UV lamp was positioned 7 cm above the solution surface and at 7.5 cm above the photocatalyst surface. The absorption of the solutions was measured at a wavelength of 660 nm at different irradiation times; to evaluate the MB concentration changes during the experiment, the Lambert–Beer's law has been employed to calculate the concentration of the MB solution at different irradiation times.

3. Results and discussion

3.1. Structural and optical characterization

In the ideal spray pyrolysis process (low temperature CVD) the solvent vaporizes before the droplet hits the hot substrate, then the solid melts and vaporizes, the resulting vapor diffuses to the substrate following a heterogeneous reaction there [16]. The formation of TiO_2 thin films by spray pyrolysis can be described by the following pyrolytical reaction:

$$TiOAA_{2(g)} + H_2O_{(g)} \rightarrow TiO_{2(s)} + 2HAA_{(g)} \quad (1)$$

where AA means acetyl acetonate. The simultaneous pyrolysis of different compounds is called copyrolysis. Copyrolysis reactions are similar to reaction (1) using solutions of $TiOAA_2$ with different amounts of $SnCl_4$ forming TiO_2/SnO_2 films with different amounts of tin. From the EDS analysis it was found that the tin percentages in the deposited films were close to the ones in the starting solutions (see Table 1). During the spray pyrolysis process the incorporation of carbon atoms coming from neither AA or from the solvent to the films occurs and the EDS analysis reveals that the carbon content is almost constant in all deposited films; it is of around 0.6%.

From the X-ray diffraction (XRD) pattern shown in Fig. 1, the polycrystalline configuration of the TiO_2 films deposited by spray pyrolysis at $T_s = 450$ °C can be observed, the anatase phase with diffraction peaks corresponding to the (101), (200), and (211) planes have been identified. The background signal in Fig. 1 reveals the presence of amorphous component from both the glass substrate and

Table 1
Optical band gaps (E_g), interplanar distances (d_{101}), and Sn content in TiO_2/SnO_2 thin films prepared with solution of TiOAA with different amounts of $SnCl_4$ (%Sn in solution)

%Sn in solution	E_g (eV)	d_{101} (Å)	%Sn in film
0	3.26	3.507	0
5	3.25	3.520	4
9	3.13	3.520	8
13	3.02	3.520	14
17	3.02	3.534	17
20	2.95	3.534	21
40	2.98	–	42
ASTM	–	3.520	

the TiO_2 film because the film thickness is around 300 nm. The diffuse nature of the diffraction peaks indicates a poor crystallinity with very small crystallites in the nanometer scale. The mean size of the crystalline particles was obtained from the XRD pattern using the Scherrer's formula yield values of 15–20 nm; suggesting that nanostructured TiO_2 thin films can be prepared by spray pyrolysis at this substrate temperature.

In this work nanocrystalline TiO_2 films of anatase phase were obtained at relatively low temperatures from alcoholic solutions of TiOAA. For comparative purposes, Abou-Helal et al. [17] using the same technique starting form titanium (IV) isobutoxide solutions have reported partially crystallized TiO_2 films at temperatures as high as 550 °C whereas in this work it has been found that polycrystalline films can be prepared at relatively low T_s (450 °C) from TiOAA solutions. Using a compound with a covalent bond between oxygen and titanium as a starting material and with an improved spraying procedure that consists in to keep the substrate temperature at a constant value during the film deposition, nanocrystalline films have been obtained at lower substrate temperature than those reported in literature [17].

Fig. 2 shows the XRD patterns of TiO_2/SnO_2 thin films with different amounts of tin and thicknesses of about 300 nm. Partially crystallized films in the anatase phase having an orientation along the plane (101) were obtained by using the solutions with %Sn=5, 9, 13, 17, and 20. Only for %Sn=20 a low intensity DRX peak can be observed between 26° and 29° which corresponds to the (111) diffraction plane of rutile SnO_2 nanocrystals (see arrows in Fig. 2). Special attention was devoted to the d_{101}, interplanar distances in order to observe changes in this parameter as the tin content was changed in the starting solution. The pure TiO_2 film exhibit a d_{101}=3.507 Å whereas TiO_2/SnO_2 layers present inter-planar distances between 3.52 and 3.534 Å, showing higher values at high SnO_2 content (see Table 1). The incorporation of Sn(IV) ions to the TiO_2 films, causes an increase in d_{101}, since Sn(IV) ions are bigger than those of Ti(IV); the ionic radii are 83 pm and 74.5 pm, respectively [18]. From the XRD patterns, it was found that the films prepared with %Sn=40 were amorphous due to the strong distortion of the crystalline lattice of anatase TiO_2 (spectrum is not shown). We found that the prepared TiO_2/SnO_2 thin films with %Sn=5–20, present a nano-structured configuration with crystalline particle sizes running from 15 to 20 nm, which were calculated using the Scherrer's formula. Similar to the XRD pattern of TiO_2 layers, the XRD patterns presented in Fig. 2 corresponding to TiO_2/SnO_2 thin films show backgrounds corresponding to amorphous components from the substrate and from noncrystalline TiO_2 and SnO_2 solids.

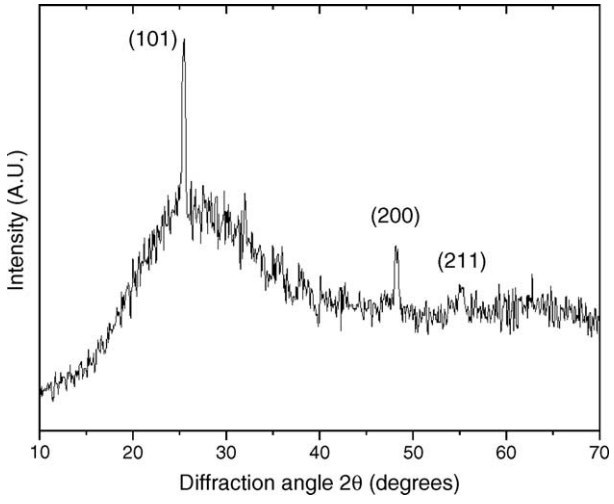

Fig. 1. X-ray diffraction (XRD) pattern of a TiO_2 thin film prepared at T_s=450 °C by spray pyrolysis method.

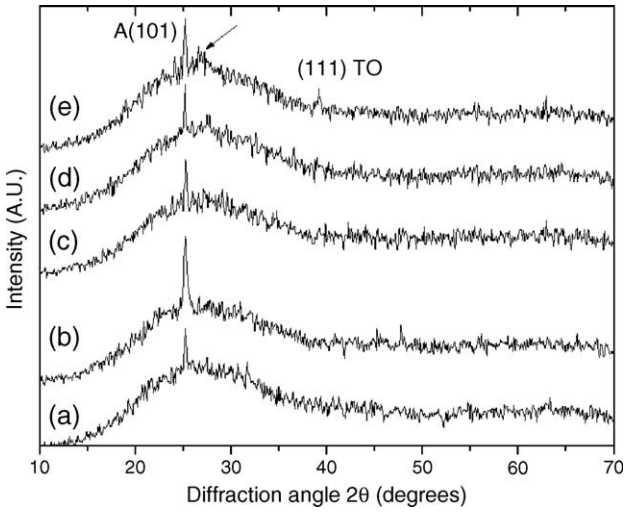

Fig. 2. XRD patterns for TiO_2/SnO_2 thin films. A — are the anatase peaks and TO — corresponding to tin oxide diffraction peak, arrows indicate the development of the SnO_2 phase. (a) %Sn=5, (b) %Sn=9, (c) %Sn=13, (d) %Sn=17, and (e) %Sn=20.

The UV–Visible absorption spectra shown in Fig. 3 reveal that the TiO_2 and TiO_2/SnO_2 films do not absorb practically in the range from 450 to 1100 nm and exhibit a very intense absorption band below of 400 nm showing a red shift of the TiO_2/SnO_2 absorption peak respect for TiO_2 films. The band gap (E_g) was obtained from the absorption spectra using the approximation reported by D. Mardare et al. [19] to calculate the absorption coefficient $\alpha(\lambda)$.

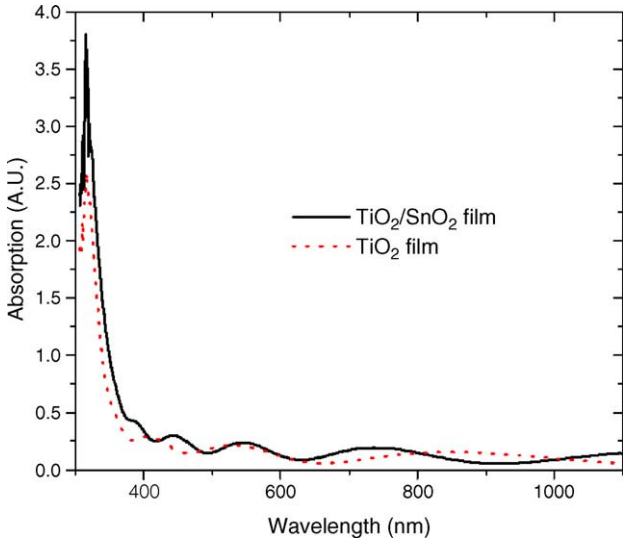

Fig. 3. UV–Visible absorption spectra of TiO_2 and TiO_2/SnO_2 (%Sn=9) thin films.

Assuming an indirect optical transition, $\alpha(\lambda)^{1/2}$ was plotted as a function of the photon energy ($h\nu$), the linear part of those graphs yields the optical gap (E_g) when $\alpha(\lambda)=0$. For TiO_2 films we found an $E_g \sim 3.25$ eV, this value is very close to those reported in the literature for sputtered titanium oxide films in the anatase phase (3.20 eV) [19]. Also, it was found that the E_g shows a decrease as the tin content in the films increases, this behavior is similar to that found by Zheng et al. [14] in TiO_2 films with implanted tin ions (TiO_2:Sn thin films).

From SEM studies it was found that TiO_2 films show intergranular spaces and discontinuities with slightly defined grains, see Fig. 4(a). On the other hand, when the Sn content is increased, the surface displays a low porous structure with a particle size of around 100 nm, see Fig. 4(b). Fig. 4(c) shows the AFM image of the surface of a TiO_2/SnO_2 film showing a root mean square (RMS) roughness of 247 Å, with a distribution of particle size of about 40–60 nm. AFM images indicate that the films are not continuous showing some surface porosity, which make them adequate for photocatalytic applications.

3.2. Photocatalytic activity

When a semiconductor catalyst is photo-excited an electron and a hole are produced, the photon energy should be equal or greater than the semiconductor energy gap (for example, $h\nu > 3.26$ eV for TiO_2 thin films and $h\nu > 3.13$ for TiO_2/SnO_2 thin films with %Sn=9). The electron-hole pair may give raise to reductive and oxidative reactions respectively. But there are recombination processes that reduce the photocatalytic efficiency of the films. As is reported here, the TiO_2/SnO_2 films present a mixture of partially crystallized Sn:TiO_2 phase with an amorphous component formed by both TiO_2 and SnO_2 phases. The method used to improve the PA consist in changing the band gap to smaller values thereby increasing the amount of electron-hole pairs when photons with energy of 3.25 and 3.39 eV impinge on the surface of photocatalyst. Also, there is a suppressing of the recombination process by

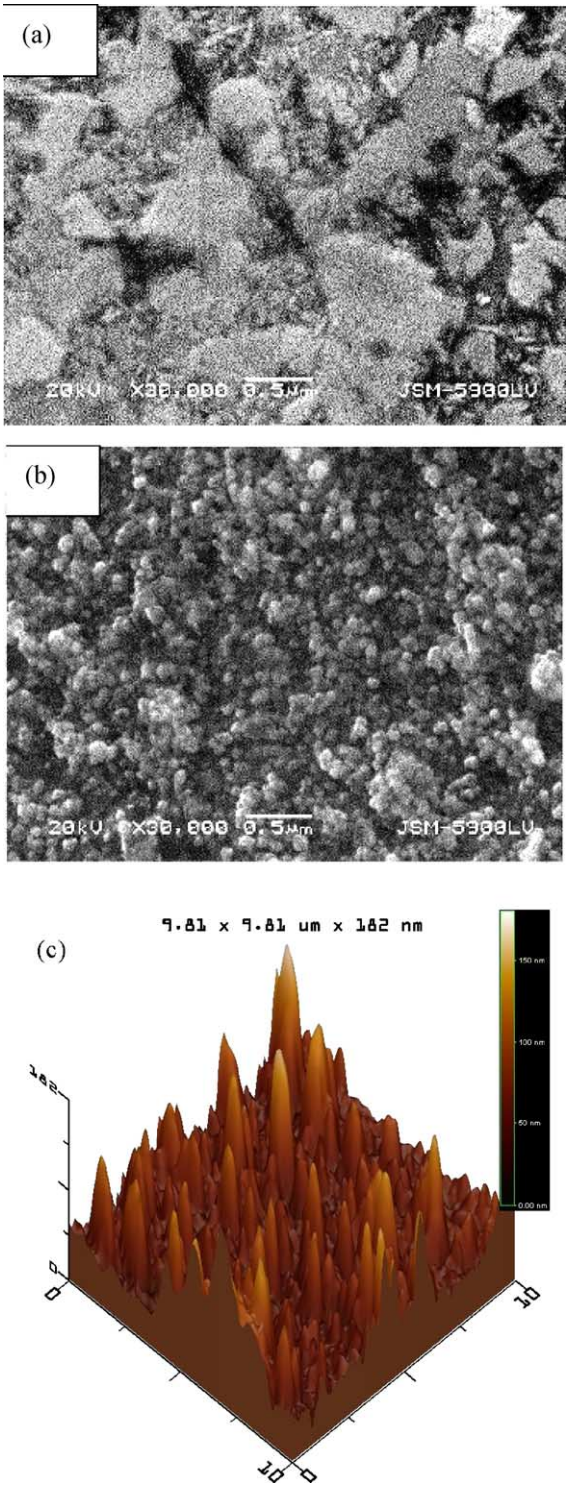

Fig. 4. Surface images obtained with: (a) SEM of a TiO_2 thin film prepared at T_s=450 °C. (b) SEM of a TiO_2/SnO_2 thin film with %Sn=9 in the starting solution. (c) AFM of a TiO_2/SnO_2 thin film with %Sn=9 in the starting solution.

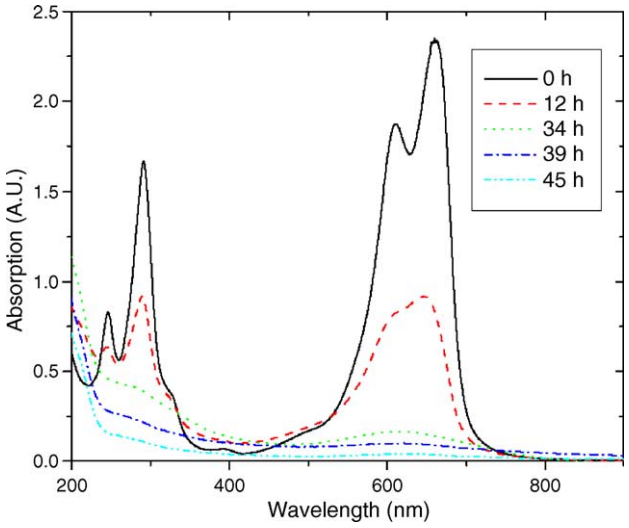

Fig. 5. Absorption spectra of MB at different irradiation times with a TiO_2/SnO_2 thin film dipped in the solution.

coupling two different semiconductors with dissimilar Fermi levels [11,13,15]. In aqueous solution, dissolved oxygen acts as an electron sink and water reacts with a hole [1]. In the later reaction a hydroxyl radical may be obtained:

$$H_2O + h^+ \rightarrow \cdot OH + H^+. \quad (2)$$

The very high oxidizing capacity of the hydroxyl radical enables it to react with most organic compounds dissolved in water. The photocatalytic activity of the thin films was characterized with the degradation of the MB compound. Fig. 5 shows the absorption spectra of the MB solution at different irradiation times with a TiO_2/SnO_2 (%Sn=9) thin film dipped in the solution; this figure shows that the absorption at 290 and 650 nm decreases when the irradiation time increases due to oxidation of the MB molecule (there is a increase in the electron deficiency and a break-down of MB). Whereas, at about 200–240 nm the absorption of the solution increases due to the creation of the degradation products such as amines and thiols. The organic degradation products were identified using ^1H NMR. Five experiments with TiO_2/SnO_2 thin film photocatalyst were made during 40 h, the resulting solutions were concentrated by evaporation of the solvent to 1 mL, the concentrated solution was mixed with deuterium oxide (D_2O), 99% deuterated, from Aldrich Chemical Company Inc. and then measured in a NMR spectrometer. The measurement was done in a BBI 400 MHz SB 5 mm with z-gradient probe; the frequency for ^1H was 400.13 MHz. The resulting spectrum is shown in Fig. 6, showing peaks (from low field to high field) at 2.6 for methylamine hydrochloride, 2.5 for dimethylamine hydrochloride, and 1.8 and 1.2 for methanethiol. The peaks mentioned above match well with the standards reported in the integrated spectral data base system for organic compounds (SDBS) [20].

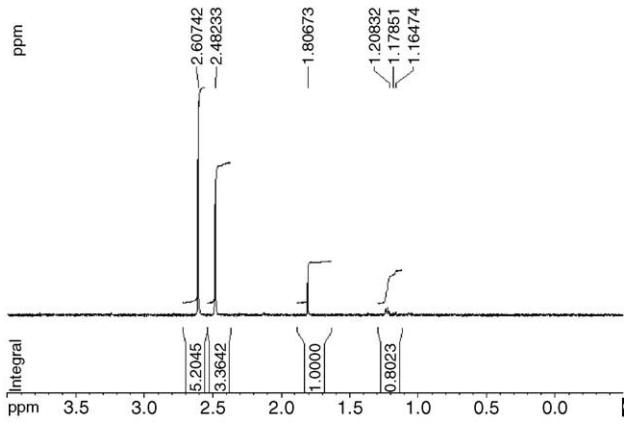

Fig. 6. ^1H NMR spectrum of the degradation products of the photocatalytic reaction, see text for details.

When the irradiation time increases, the absorption in the UV range mentioned above decreases due to the oxidation of the small organic compounds to carbon dioxide, as it is indicated in the mineralization reaction of MB (3). Therefore, the oxidation of MB to mineral compounds is possible by photocatalysis with TiO_2 and TiO_2/SnO_2 thin films.

$$C_{16}H_{18}N_3S{\cdot}Cl + 24O_2 \rightarrow 16CO_2 + 6HO_2 + 3NH_4^+ + SO_4^{2-} + Cl^- . \quad (3)$$

Fig. 7 shows changes in MB concentration with increasing irradiation time by pure TiO_2 and TiO_2/SnO_2 thin films. From this figure we can conclude that the photocatalytic reactions follow a pseudo- first order kinetics for pure and alloyed films. The degradation efficiency for all TiO_2/SnO_2 thin films is higher than that of pure titanium oxide films, showing a maximum for TiO_2/SnO_2 films with

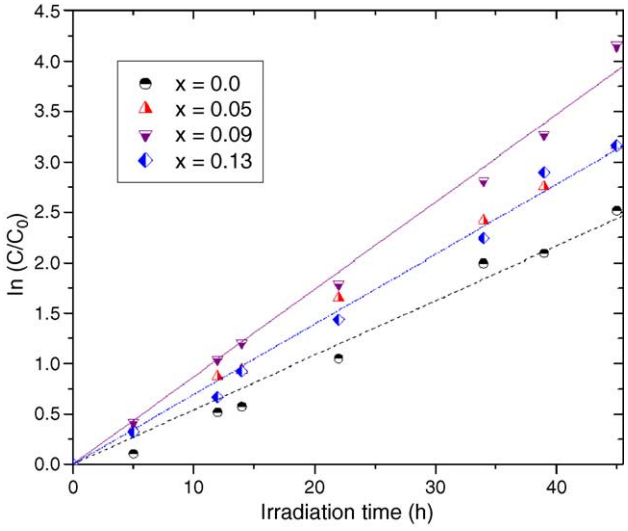

Fig. 7. Photocatalytic degradation of methylene blue by various TiO_2/SnO_2 thin film photocatalyst.

%Sn=9. This behavior is due to different factors such as: the increase in the surface area with the increase in the tin content, the presence of two semiconductors with different Fermi levels, and smaller energy gap than one exhibited by TiO_2 films; these improve both the separation and the photo-generation of electron-hole pairs. Also, it has been reported [14] that the tin ions have more affinity to the adsorption of hydroxyl ions yielding as a result an increase in the surface hydroxyl groups that can be trapped in the photo-generated holes producing very reactive hydroxyl radicals. Also it was found that in the UV range there is an increase in the absorption of the solution during the photocatalytic reaction; this behavior is due to the creation of the degradation products (organic compounds with one or two carbon atoms); that have been identified by ^1H nuclear magnetic resonance (NMR) as dimethylamine hydrochloride, methanethiol, and methylamine.

4. Conclusions

Polycrystalline films in anatase phase have been prepared from TiOAA at relatively low substrate temperatures by the spray pyrolysis method. The copyrolysis of TiOAA and $SnCl_4$ solutions causes the insertion of Sn(IV) ions in the anatase lattice producing different modifications in the physical properties of the partially crystallized TiO_2 films. It was observed that at low concentrations of tin in the starting solution, the lattice parameter increases as the amount of Sn(IV) increases. At high tin concentrations (%Sn=40), the structure is predominantly amorphous. When the concentration of tin in the solution was 0.2 we found a small amount of rutile SnO_2 crystalline phase in the thin films. As the amount of Sn in the starting solution is increased up to %Sn=9, the photocatalytic activity increases, suggesting a more efficient separation of photo-generated electron-hole pairs.

Acknowledgements

The authors acknowledge valuable scientific discussions and technical support of Dr. Alfredo Gomez, Ivan Puente, Manuel Aguilar, Carlos Magaña, Juan G. Morales, and Alexander Malik. This work was supported by DGAPA through the projects IN 109500 and IN 103705.

References

[1] J.-M. Herrmann, Catal. Today 53 (1999) 115.
[2] U. Kirner, K.D. Schierbaum, Sens. Actuators, B 1 (1990) 103.
[3] G.P. Burns, I.S. Baldwin, M.P. Hastings, J.G. Wilkes, J. Appl. Phys. 66 (1989) 2320.
[4] R. Cinnsealach, G. Boschloo, S.N. Rao, Sol. Energy Mater. Sol. Cells 57 (1999) 107.
[5] F. Lapostolle, A. Billard, V. von Stebut, Surf. Coat. Technol. 135 (2000) 1.
[6] F. Zhang, N. Huang, P. Yang, X. Zeng, Y. Mao, Z. Zheng, Z. Zhou, X. Liu, Surf. Coat. Technol. 84 (1996) 476.
[7] H. Bach, D. Krause, Thin Films on Glass, Springer-Verlag, Berlin, 1997.
[8] M.R. Hoffmann, S.T. Martin, W. Choi, D.W. Bahnemann, Chem. Rev. 95 (1995) 69.
[9] A.L. Linsebigler, G.Q. Lu, J.T. Yates, Chem. Rev. 95 (1995) 735.
[10] X.Z. Li, F.B. Li, C.L. Yang, W.K. Ge, J. Photochem. Photobiol., A Chem. 141 (2001) 209.
[11] K. Vinodgopal, P.V. Kamat, Environ. Sci. Technol. 29 (1995) 841.
[12] Y.R. Do, W. Lee, K. Dwight, A. Wold, J. Solid State Chem. 108 (1994) 198.
[13] J. Lin, J.C. Yu, J. Lo, S.K. Lan, J. Catal. 183 (1999) 368.
[14] S.K. Zheng, T.M. Wang, W.C. Hao, R. Shen, Vacuum 65 (2002) 155.
[15] Y. Cao, W. Yang, W. Zhang, G. Liu, P. Yue, New J. Chem. 2 (2004) 218.
[16] W. Siefert, Thin Solid Films 120 (1984) 275.
[17] M.O. Abou-Helal, W.T. Seeber, Appl. Surf. Sci. 195 (2002) 53.
[18] J.E. Huheey, Inorganic Chemistry: Principles of Structure and Reactivity, Harper and Row, New York, 1972.
[19] D. Mardare, M. Tasca, M. Delibas, G.I. Rusu, Appl. Surf. Sci. 156 (2000) 200.
[20] www.aist.go.jp/RIODB/SDBS/.